



Accelerated Thermal Aging Test for Predicting Lifespan of Urethane-Based Elastomer Potting Compound

Min-Jun Gim[‡], Jae-Hyeon Lee[‡], Seok-Hu Bae, Jung-Hwan Yoon, and Ju-Ho Yun[†]

Chemical Materials R&D Center, Korea Automotive Technology Institute, 303 Pungse-ro, Pungse-myeon, Dongnam-gu, Cheonan-si, Chungnam 31214, Republic of Korea

(Received April 15, 2024, Revised June 26, 2024, Accepted June 28, 2024)

Abstract: In the field of electronic components, the potting material, which is a part of the electronic circuit package, plays a significant role in protecting circuits from the external environment and reducing signal interference among electronic devices during operation. This significantly affects the reliability of the components. Therefore, the accurate prediction and assessment of the lifespan of a material are of paramount importance in the electronics industry. We conducted an accelerated thermal aging evaluation using the Arrhenius technique on elastic potting material developed in-house, focusing on its insulation, waterproofing, and contraction properties. Through a comprehensive analysis of these properties and their interrelations, we confirmed the primary factors influencing molding material failure, as increased hardness is related to aggregation, adhesion, and post-hardening or thermal-aging-induced contraction. Furthermore, when plotting failure times against temperature, we observed that the hardness, adhesive strength, and water absorption rate were the predominant factors up to 120 °C. Beyond this temperature, the tensile properties were the primary contributing factors. In contrast, the dielectric constant and loss tangent, which are vital for reducing signal interference in electric devices, exhibited positive changes(decreases) with aging and could be excluded as failure factors. Our findings establish valuable correlations between physical properties and techniques for the accurate prediction of failure time, with broad implications for future product lifespans. This study is particularly advantageous for advancing elastic potting materials to satisfy the stringent requirements of reliable environments.

Keywords: urethane, elastomer, potting, accelerated aging test, lifespan, arrhenius equation

Introduction

Recently, the automotive industry is undergoing a significant shift from internal combustion engine vehicles to electric-powered ones.^{1,2} With the increasing number of electronic components, there is a growing demand for these components to improve user convenience.³ Therefore, there is an urgent need to significantly enhance the functionality and operational conditions of these components. In particular, the shift towards electric vehicles and the introduction and expansion of driving convenience features such as advanced driver assistance systems (ADAS) underscore the vital role of both performance and reliability in the electronic components that control them.⁴ This is because vehicle operation is increasingly reliant on electric devices rather than human intervention, and any failure of these components directly impacts driver safety.⁵ These electrical components

are directly integrated on a printed circuit board (PCB) and are safeguarded from environmental factors, including moisture, dust, vibration, and extreme temperatures, through encapsulation in organic polymers.⁶⁻⁹ This process, known as potting, involves filling and covering the electronic asset with liquid polymer compounds, which are then cured to improve both protection and reliability. Therefore, since the reliability of the device can depend greatly on the properties of the potting material, it is very important to prevent unexpected large accidents by predicting the lifespan of these materials in advance.¹⁰

Potting enhances its functionality through the incorporation of composite materials, including inorganic particles and fillers, with organic polymer materials serving as the primary components.¹¹⁻¹³ However, it is important to note that these organic polymers can undergo aging due to external environmental conditions such as temperature, humidity, direct sunshine, or physical stresses (mechanical stress, bending, wear, etc.). This aging process can lead to the deterioration of physical properties, potentially resulting in product failure

[†]Corresponding author E-mail: jhyun@katech.re.kr

[‡]The authors contributed equally to this work

due to an inability to meet the minimum required performance standards. To accurately assess the lifespan of a product, it is ideal to estimate it by subjecting the product to actual environment conditions. However, this approach is often time-consuming and challenging, as it is difficult to simulate the actual operational environment under various conditions. Consequently, accelerated life tests (ALT) are being explored to expedite the determination of a product's lifespan.¹⁴⁻¹⁷ These involve subjecting the product to harsh conditions that intensify the key factors affecting its deterioration, allowing for a quicker assessment of its durability.

The basic model for determining temperature-related acceleration factors in polymer materials generally follows the Arrhenius Law.^{15,16} This entails exposing the materials to harsher conditions than their nominal environment to accelerate potential failures. The relationship between product lifespan and stress is then estimated by analyzing the observed results obtained under these accelerated conditions. This outcome is then extrapolated to predict the product's lifespan under its actual usage environment. The Arrhenius model, which forecasts service life through an accelerated temperature-based life test, is represented by the equation (1).

$$k = Ae^{-\frac{E_a}{RT}} \quad (1)$$

Where k is the reaction rate or degradation rate, A is a materials and environment related constant, E_a is the energy of activation, R is the universal gas constant (8.3143 J/mol K), and T is the absolute temperature in degrees Kelvin. In this equation, the reaction necessitates a minimum amount of energy, referred to as activation energy. When a large number of molecules possess energy exceeding this minimum threshold, the reaction rate escalates. With higher temperatures, more molecules surpass the activation energy requirement, resulting in an increased reaction rate. Equation (2) can be derived by taking the natural logarithm of both sides of equation (1).

$$\ln k = -\frac{E_a}{RT} + \ln A \quad (2)$$

Equation (2) shows that there is a linear relationship between $\ln k$ and $1/T$, allowing the activation energy and reaction rate to be determined by obtaining the slope and intercept from this linear relationship. Based on this

Arrhenius equation, assuming that a failure occurs when physical properties reach a specific threshold, the connection between lifetime and test temperature can be expressed using Equation (3).

$$\ln t = -\frac{E_a}{RT} + \ln B \quad (3)$$

Where t is lifetime, and B is a constant. Thus, by substituting the failure lifetime obtained for each temperature through ALT experiments into this equation, it becomes feasible to predict the performance duration at the desired temperature.

In this study, we developed a potting material specifically designed to protect antennas that support 5G integrated ultra-wideband technology in connected cars. These vehicles enable interactive Internet and mobile services, bridging next-generation information and communication technologies with automotive systems. The antenna, shielded by the potting material, is positioned closer to the surface of the vehicle to facilitate seamless communication with external entities, such as vehicles-to-vehicles, vehicles-to-infrastructure, vehicles-to-network, and vehicles-to-home interactions, all operating within the vehicles-to-everything (V2X) paradigm.¹⁸ As a result, due to heightened exposure to external conditions in comparison to other electronic components, the potting material's service life significantly influences the overall functionality and durability of connected cars, including the antenna. We employed a conservative approach to estimate the lifespan of the potting material. It was categorized into key factors, including shrinkage, water resistance, and insulation, to account for aging. Subsequently, we conducted the ALT using the Arrhenius equation to evaluate these factors and calculate and compare the expected failure times based on the operating temperature. For this, the calculation and discussion of failure times were not limited to individual factors but encompassed the consideration of multiple factors in combination. This approach allowed us to identify the predominant failure factor at specific operating temperatures. By adopting this method, we believe that we can provide a conservative and more accurate prediction of the service life of electronic component protection materials, which play a crucial role in ensuring safety, reliability, and functionality in the evolving next-generation automotive field. Ultimately, this can assist consumers in enhancing safety and reliability aspects related to the longevity of critical components, thus contributing to the advancement of the automotive industry.

Experimental

1. Materials and Sample preparation

We used a urethane-type material based on high-functional butadiene rubber developed by ESPchem (Korea). The primary material and curing agent were mixed at a ratio of 100:25. The primary material includes hydroxyl-terminated polybutadiene (HTPB, DL chemicals), a polyol, a variety of additives, and inorganic fillers. The curing agent primarily comprises isocyanate functional groups, which can react with the hydroxyl group of polyol or butadiene to create polyurethane (PU). After mixing the two materials using a paste mixer for approximately 10 minutes, we poured the mixture into a mold to create the specimen. Subsequently, the specimen was cured at 60°C for 24 hr before being processed to meet the measurement requirements.

2. Characterization

The ALT test items are tensile strength, elongation, shear strength, hardness, water absorption rate, dielectric constant, and dielectric loss. For tensile strength and elongation, a universal testing machine (AG-50kNXD, SHIMADZU) was used by processing the specimen to conform to the KSM ISO 527-2 standard. The specimen was manufactured to comply with KS M ISO 4587 for shear strength, and PBT-GF30% (TECADUR PBT GF30 natural, Ensinger) was used as a substrate. The hardness was prepared in compliance with KS-ISO 868, and Durometer type A (ASKER) equipment was used. The water absorption rate was tested in compliance with ASTM D570-98, and data were collected based on 1 V, 100 kHz using the LCR meter (E4980AL, Keysight) equipment for dielectric constant and dielectric loss tangent. To analyze the aging mechanism, we conducted attenuated total reflection (ATR) fourier transform infrared (FTIR) spectroscopy (Spectrum 100, PerkinElmer) and measured the roughness average (Ra) of the surface (OLS5000, OLYMPUS). The acceleration conditions for the ALT test were 120°C, 140°C, 160°C, and physical properties were measured at intervals of 0 hr, 48 hr, 96 hr, 168 hr, 336 hr, and 672 hr. To determine the appropriate acceleration temperature, thermogravimetric analysis (TGA) was conducted using a TGA 4000 (PerkinElmer) instrument. The specimen was first stabilized at 40°C for 10 min, then heated from 40°C to 800°C at a rate of 5°C/min.

Results and Discussion

To determine the failure time using the Arrhenius technique, we derive a linear equation by extrapolating from a graph that incorporates the reciprocal of the absolute temperature and the natural logarithm of the failure time. Following this, the failure time is recalculated for various aging temperatures. Ensuring the reliability of the linear equation requires considering at least three points within the aging acceleration temperature range. TGA was conducted to determine the appropriate acceleration temperature for aging. When measuring the thermal decomposition temperature of the cured potting specimen, the first thermal decomposition occurred at approximately 275°C, with gradual decomposition starting from 200°C. Therefore, conducting long-term aging tests at temperatures above 200°C is not suitable (See Figure 1). Aging occurs too rapidly above 160°C, making it difficult to plot the results. Conversely, below 100°C, it takes a very long time to reach the failure time. Therefore, we selected three temperature ranges: 120°C, 140°C, and 160°C, setting intervals of 20°C to give distinct thermal histories for each range. Physical property variations at each temperature are recorded by placing specimens in the designated temperature chambers and taking them out at regular intervals for physical property measurements. When the alterations in physical properties reach a predefined threshold, it is considered a failure, and this threshold is referred to as the lifetime limit. Setting the lifetime limit is first and foremost crucial in this procedure. Following the guidelines outlined in ASTM D 2000, we have established the lifetime limit based on the point where initial properties deviate by 30% for tensile strength, 50% for elongation at break, and ± 15 for hardness.¹⁵ For shear strength or water absorption rate, we

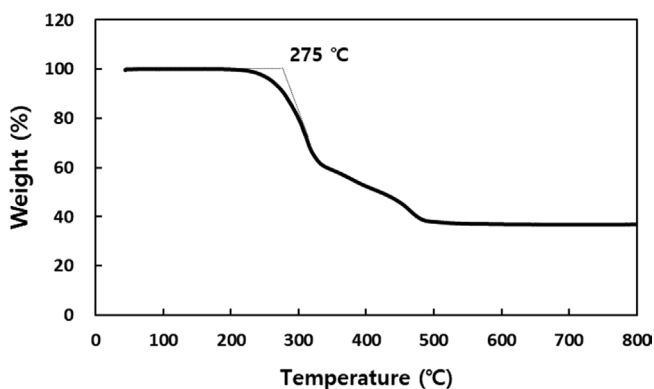


Figure 1. Thermogravimetric analysis data for a pristine sample.

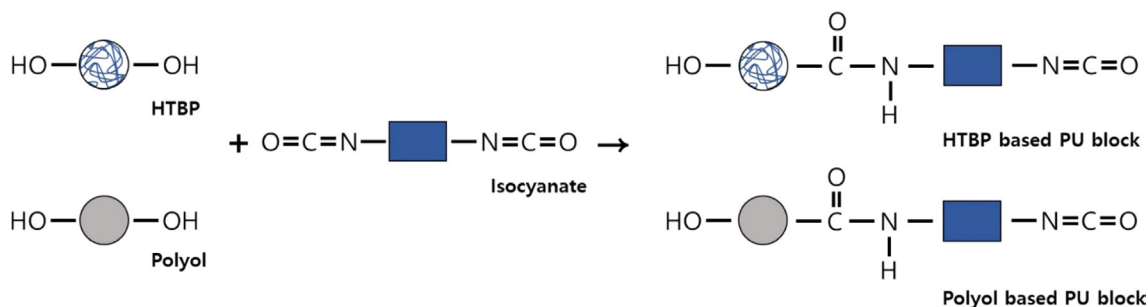
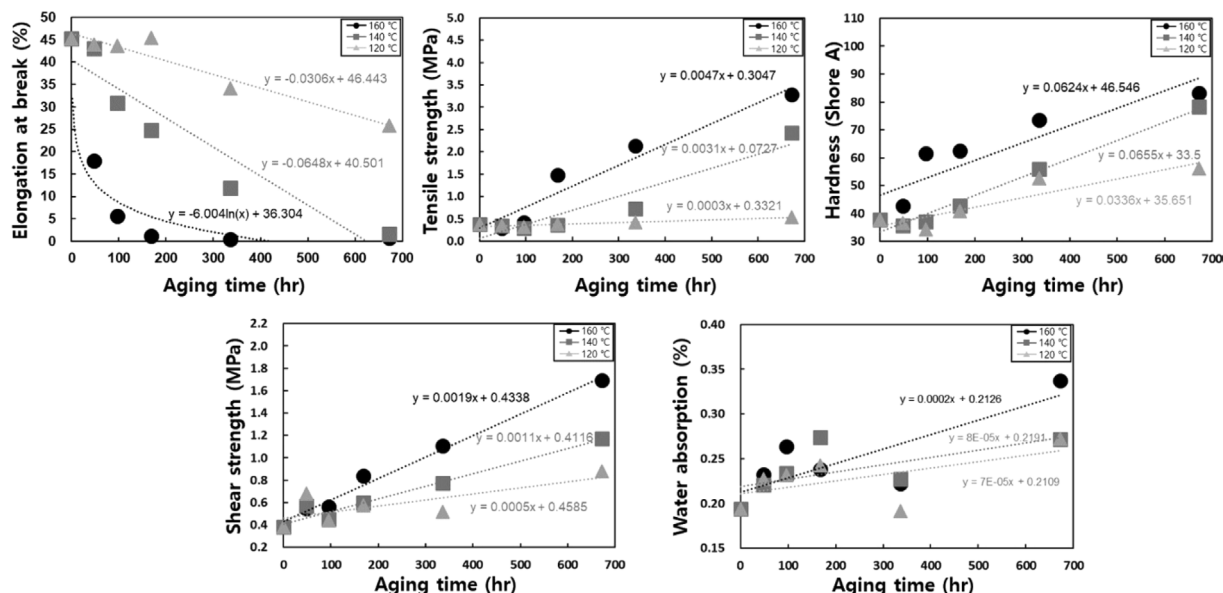
Table 1. Initial Physical Properties, Lifetime Limits, and Failure Times for Each Test Item Under Accelerated Temperatures

Physical properties		Elongation at break (%)	Tensile strength (MPa)	Hardness (Shore A)	Shear strength (MPa)	Water absorption (%)
Pristine property		45.19	0.38	38	0.38	0.19
Lifetime limit		22.60	0.50	53	0.57	0.29
Failure time (hr)	120°C	779	556	516	231	1147
	140°C	276	137	298	148	982
	160°C	10	41	103	74	393

adhere to the recommendations stipulated in UL standards, where electronic devices or plastic performance is advised to maintain 50% of the initial performance after more than 100,000 hr of use.¹⁹ As per these regulations, we set the lifetime limit with a 50% variation in properties (See Table 1).

In Figure 1, the data extracted based on aging time undergo regression analysis for each physical property, resulting in the

derivation of suitable regression equations. By inserting the lifetime limit for each physical property into the variable (y) within the respective regression equations and calculating the time variable (x) required to reach the specified lifetime limit in reverse, the failure time at each accelerated temperature can be determined, as shown in Table 1. The potting material currently in development is formulated by reacting polyol, which serves as the soft segment, with isocyanate,

**Figure 2.** Schematics of polyurethane formation through the reaction of polyol with isocyanate and HTPB with isocyanate.**Figure 3.** Variation of physical properties under aging conditions.

responsible for the hard segment, as part of the PU series. Hydroxyl-terminated polybutadiene (HTPB), employed as another soft segment of PU, can undergo a reaction with isocyanate, leading to outstanding properties, including low surface energy, flexibility at low temperatures, high electric insulation, elevated viscoelasticity, tenacity, and hydrolytic stability²⁰ (See Figure 2). However, as the potting material ages under high temperatures, the behavior of all physical factors indicates an increase in hardness (See Figure 3). Thermal energy forms residual reactive sites, creating new crosslinks that diminish elastic force. Simultaneously, molecular distances contract through the diffusion of molecules during the crosslinking process. This phenomenon aligns with the typical thermal aging behavior observed in elastic rubber (HTPB) or elastomer (PU).²¹ Additionally, the packing density of the bulk aromatic blocks, responsible for the hard segment in PU, increases. Consequently, elasticity diminishes due to alterations in the intermolecular packing structure induced by additional crosslinking and heat. This results in a reduction in elongation, accompanied by an increase in tensile strength and hardness, as shown in Figure 3. Based on the FTIR results, it is evident that the changes in properties due to thermal aging are attributed to physical factors rather than the thermal decomposition of PU linkages, because no newly formed peaks were observed when comparing FTIR spectra before and after aging (See Figure 4). The thermal decomposition of PU linkages typically produces Isocyanate (-NCO) and Amine (-NH) groups as byproducts.²² However, since no new peaks around 2260 cm^{-1} for -NCO stretch and $3400\text{-}3500\text{ cm}^{-1}$ for -NH stretch were observed in the FTIR results, thermal decomposition was not considered a factor in this study. As thermal aging progresses, the overall peak intensity decreases due to an increase in surface roughness caused by the physical degradation of the material, which in turn increases light scattering. The enhancement of crosslinking or improvement in intermolecular packing density occurs not only in the bulk region but also at the interface with the substrate, contributing to an overall increase in shear strength. Regarding the water absorption rate, measured by weighing the specimen before and after immersion in water, it increases with aging. On the surface, stress is generated in a mutual direction parallel to the stress in the inner direction due to contraction, and the magnitude of the stress applied to the outside increases rather than the inside. It is unable to withstand such high stress; consequently, in order to reduce

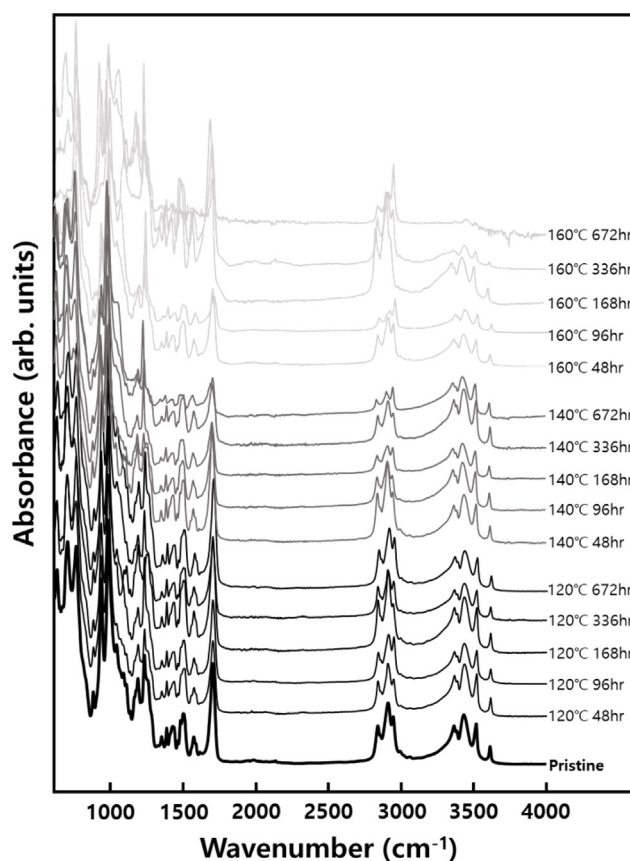


Figure 4. Attenuated total reflection-Fourier transform infrared spectroscopy spectra of pristine and thermally aged samples.

the increased stress, fine cracks occur on the surface with increased roughness (See Figure 5). These fine cracks result in moisture absorption, causing the weight of the specimen to increase as it ages.

The main purpose of potting materials is to offer physical protection to circuits while also playing a crucial role in electrical insulation to minimize signal interference among highly integrated chips. For this reason, we also examined the dielectric behavior. However, the dielectric constant and dielectric loss tangent decreased as aging progressed. These changes had a positive impact on the electrical insulation of the device, leading us to exclude them as contributing factors to failure. In contrast to physical elements, dielectric behavior exhibits an inflection point where characteristics initially increase and then decrease with the progression of aging. Thermal energy induces additional crosslinking, and the strengthened bonding force promotes electron movement between the chains, leading to an increase in dielectric constant and dielectric loss (See Figure 6). However, as

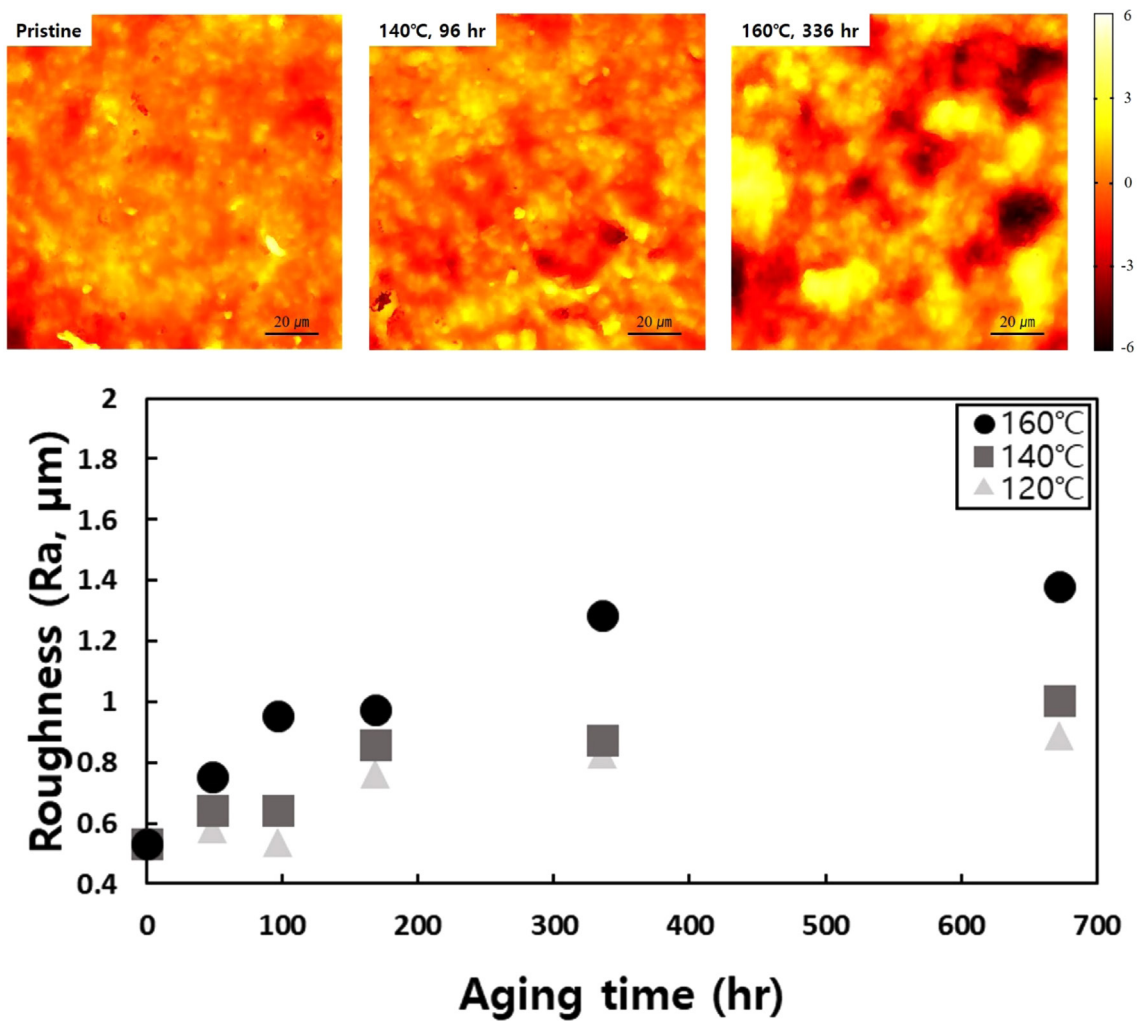


Figure 5. The surface roughness of pristine and thermally aged samples.

crosslinking increases further due to additional heat aging and the packing density of the hard segment rises, molecular motion is suppressed, leading to a decrease in electrical conduction or polarization. Consequently, there is a gradual decline in dielectric constant and dielectric loss. This aligns

with the mechanism described in low dielectric substance liquid crystal polymer for next-generation communication devices.²³

The Arrhenius plot is generated using the failure time data extracted from Table 1 at the three ALT temperatures

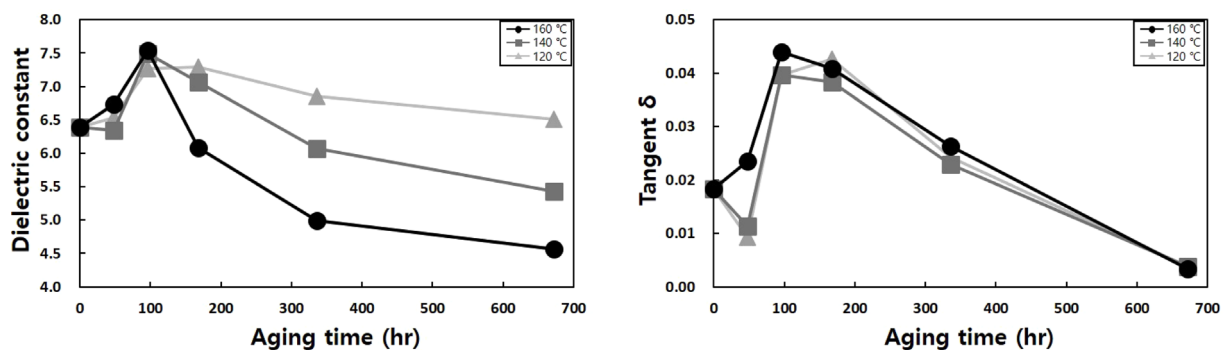


Figure 6. Variation of dielectric properties under aging conditions.

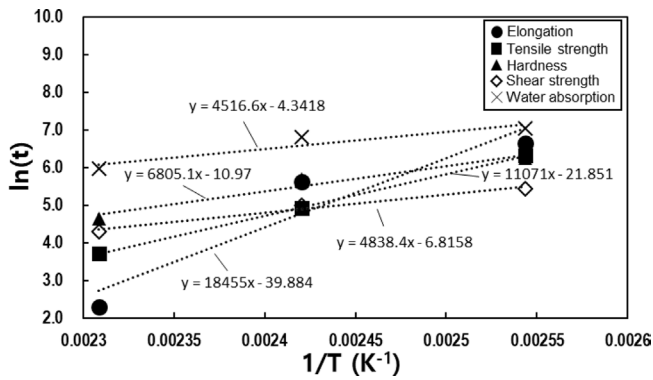


Figure 7. Arrhenius plots for lifetime as a function of temperature.

determined through regression analysis (refer to Figure 7). This plot takes the form of Equation 3, representing a linear relationship between the reciprocal of the absolute temperature and the failure time (hours) taken by the natural logarithm. To establish a highly reliable linear regression equation, it is essential to perform ALT at least three temperature points. The resulting Arrhenius equation for each physical property is presented in Table 2. Additionally, by incorporating the reciprocal of the absolute temperature at 25°C into the variable x , the failure time at room temperature can be calculated. Based on the results, the factors that fail at room temperature, listed in order of significance, are shear strength, water absorption, hardness, tensile strength, and elongation. However, upon analyzing the data, it becomes evident that tensile strength and elongation cannot be considered the primary contributors to failure at room temperature, as they are indicative of a representation exceeding 100 years of use.

However, in practical applications, the product is not employed under isothermal conditions. Circuits with an exceptionally high degree of integration generate significant heat during operation, and devices designed for outdoor use are exposed to increasingly challenging environments. Therefore, it becomes imperative to assess not only room temperature but also a broader range of usage conditions.

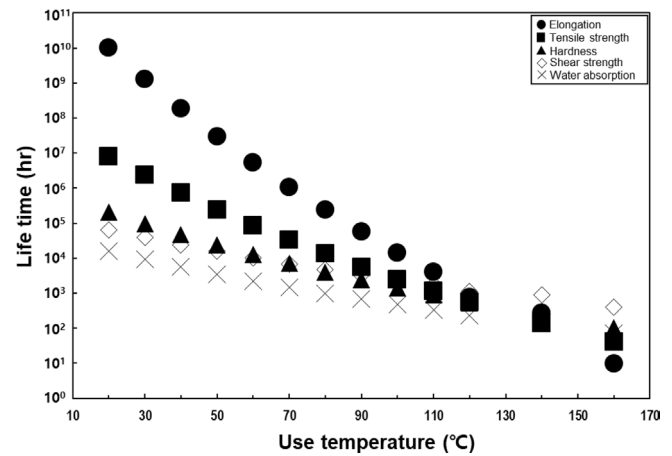


Figure 8. Failure time variation with respect to use temperature for each physical property.

To achieve this, the failure time at various temperatures for each testing item was calculated and schematized using the Arrhenius equation in Table 2. When examining the failure time based on the temperature for each physical property, it is observed that the failure of shear strength, water absorption, and hardness occurs more rapidly before approximately 120°C. However, above 120°C, there is a reversal, with the physical properties of tensile strength and elongation reaching failure faster (See Figure 8). Therefore, when observing the failure time across the entire temperature range, it becomes evident that the dominant factors causing product failure in mild and harsh environments are different. This approach can serve as a tool to appropriately identify areas for improvement to enhance the usage cycle based on the thermal history environment that the actual product experiences.

Conclusions

Based on the ALT experimental technique, a study was conducted on the potting material designed to protect communication components in connected cars equipped

Table 2. Arrhenius Equations for Each Testing Item and Estimated Lifetime at Room Temperature

Physical properties	Arrhenius equation	Estimated lifetime (year) at 25°C
Elongation at break	$\ln(t) = 18455x - 39.884$	415161
Tensile strength	$\ln(t) = 11071x - 21.851$	494
Hardness	$\ln(t) = 6805.1x - 10.97$	16
Shear strength	$\ln(t) = 4838.4x - 6.8158$	1
Water absorption	$\ln(t) = 4516.6x - 4.3418$	6

with 5G integrated wideband communication technologies. The goal was to calculate the failure time based on usage temperature and identify the primary factors contributing to failure. A conservative approach was adopted to enhance the reliability of the automotive industry, foreseeing potential issues arising from electronic device malfunctions at the crossroads of vehicle electrification. By examining the correlation between various physical properties rather than focusing on individual attributes, we made predictions about the failure life of different aspects. This approach allowed us to pinpoint areas requiring specific improvements, thereby extending the product's overall service life. Based on 120°C, shear strength, water absorption, and hardness were the main causes of failure at low temperatures, and elongation and tensile strength at high temperatures were the main causes. This technique strategy can help to formulate an appropriate physical property development strategy to expand the usage cycle in consideration of the actual product usage environment.

Acknowledgements

This research was supported by the Ministry of Trade, Industry, and Energy Grant funded by the Korean Government [Project Number 20016600].

Conflict of Interest: The authors declare that there is no conflict of interest.

References

1. F. Hoefft, "Internal combustion engine to electric vehicle retrofitting: potential customer's needs, public perception and business model implications", *Transp. Res.*, **9**, 100330 (2021).
2. R. Casper and E. Sundin, "Electrification in the automotive industry: effects in remanufacturing", *J. Remanufacturing*, **11**, 121 (2020).
3. F. Arena, G. Pau, and A. Severino, "An overview on the current status and future perspectives of smart cars", *Infrastructures*, **5**, 53 (2020).
4. A. M. Khan, A. Bacchus, and S. Erwin, "Policy challenges of increasing automation in driving", *LATSS Res.*, **35**, 79 (2012).
5. I. Nastjuk, B. Herrenkind, A. B. Brendel, M. Marrone, and L. M. Kolbe, "What drives the acceptance of autonomous driving? An investigation of acceptance factors from an end-user perspective", *Technol. Forecast. Soc. Chang.*, **161**, 120319 (2020).
6. S. N. Gladkikh, E. N. Basharina, O. L. Troitskaya, S. P. Kriulina, N. V. Timoshchenko, and I. V. Nikitushkin, "Development and tests of thermally stable potting and impregnating compounds", *Polym. Sci. Ser. D*, **5**, 145 (2012).
7. H. Ardebili, J. Zhang, and M. G. Pecht, "Encapsulation technologies for electronic applications" William Andrew, 2018.
8. M. Shtein, R. Nadiv, M. Buzaglo, and O. Regev, "Graphene-based hybrid composites for efficient thermal management of electronic devices", *ACS Appl. Mater. Interfaces*, **7**, 23725 (2015).
9. C. Hu, W. Zheng, B. Zhao, Y. Fan, H. Li, K. Zheng, and G. Wang, "The effect of thermal and moisture stress on insulation deterioration law of ionic contaminated high-voltage printed circuit board of electronic power conditioner", *Energies*, **15**, 9616 (2022).
10. R. Kulkarni, M. Soltani, P. Wappler, T. Guenther, K.-P. Fritz, T. Groezinger, and A. Zimmermann, "Reliability study of electronic components on board-level packages encapsulated by thermoset injection molding", *J. Manuf. Mater. Process.*, **4**, 26 (2020).
11. G.-W. Lee, M. Park, J. Kim, J. I. Lee, and H. G. Yoon, "Enhanced thermal conductivity of polymer composites filled with hybrid filler", *Compos. Part A*, **37**, 727 (2006).
12. Y. Zhou, Y. Yao, C.-Y. Chen, K. Moon, H. Wang, and C.-P. Wong, "The use of polyimide-modified aluminum nitride fillers in AlN@PI/Epoxy composites with enhanced thermal conductivity for electronic encapsulation", *Sci. Rep.*, **4**, 4779 (2014).
13. E. J. R. Phua, M. Liu, B. Cho, Q. Liu, S. Amini, X. Hu, and C. L. Gan, "Novel high temperature polymeric encapsulation material for extreme environment electronics packaging", *Mat. Des.*, **141**, 202 (2018).
14. R. Bernstein, D. K. Derzon, and K. T. Gillen, "Nylon 6.6 accelerated aging studies: thermal-oxidative degradation and its interaction with hydrolysis", *Polym. Degrad. Stab.*, **88**, 480 (2005).
15. H. S. Lee, J. H. Do, W. Ahn, and C. Kim, "A study on physical properties and life time prediction of ACM rubber for automotive engine gasket", *Elastomers Compos.*, **47**, 254 (2012).
16. M. A. G. Silva, B. S. d. Fonseca, and H. Biscaia, "On estimates of durability of FRP based on accelerated tests", *Compos. Struct.*, **116**, 377 (2014).
17. T. K. Kang, B. I. Choi, C. S. Woo, and W. D. Kim, "Evaluation of the aging life of the rubber pad in power window switch", *Elastomers Compos.*, **54**, 351 (2019).

18. H. S. Das, M. M. Rahman, S. Li, and C. W. Tan, "Electric vehicles standards, charging infrastructure, and impact on grid integration: A technological review", *Renew. Sustain. Energy Rev.*, **120**, 109618 (2020).
19. S. Kurtz, K. Whitfield, D. Miller, J. Joyce, J. Wohlgemuth, M. Kempe, N. Dhere, N. Bosco, and T. Zgonena, "Evaluation of high-temperature exposure of rack-mounted photovoltaic modules", *In Proceedings of the 34th IEEE PVSC.*, 2399 (2009).
20. J. Li, Z. Ning, W. Yang, B. Yang, and Y. Zeng, "Hydroxyl-terminated polybutadiene-based polyurethane with self-healing and reprocessing capabilities", *ACS Omega*, **7**, 10156 (2022).
21. C.-B. Kim and S. Kim, "Study on the properties of flexible polyurethane foam at the aging condition", *KIGAS*, **16**, 123 (2012).
22. J. A. Hiltz, "Analytical pyrolysis gas chromatography/mass spectrometry (py-GC/MS) of poly(ether urethane)s, poly(ether urea)s and poly(ether urethane-urea)s", *J. Anal. Appl. Pyrol.*, **113**, 248 (2015).
23. H. Yang, G. Yuan, E. Jiao, K. Wang, W. Diao, Z. Li, K. Wu, and J. Shi, "Low dielectric constant and high thermal stability of liquid crystal epoxy polymers based on functionalized poly(phenylene oxide)", *Eur. Polym. J.*, **198**, 112378 (2023).

Publisher's Note The Rubber Society of Korea remains neutral with regard to jurisdictional claims in published articles and institutional affiliations.